Effective Utilization of in Situ Generated Hydroperoxide by a Co– SiO₂@Ti–Si Core–Shell Catalyst in the Oxidation Reactions

Meng Liu,[†,‡] Song Shi,[*,†] Li Zhao,[†,‡] Min Wang,[†] Guozhi Zhu,[†,‡] Xi Zheng,[†] Jin Gao,[†] and Jie Xu[*,†]
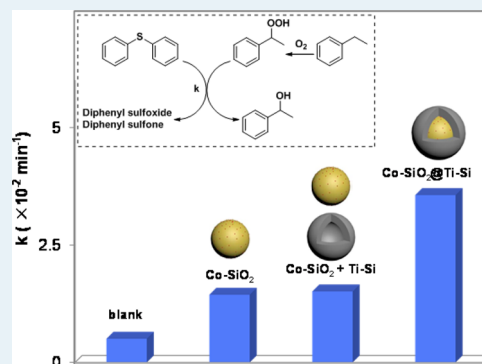
[†]State Key Laboratory of Catalysis, Dalian National Laboratory for Clean Energy, Dalian Institute of Chemical Physics, Chinese Academy of Sciences, Dalian 116023, People's Republic of China

[‡]University of Chinese Academy of Sciences, Beijing 100049, People's Republic of China

Ⓢ Supporting Information

ABSTRACT: A core−shell catalyst (Co−SiO₂@Ti−Si) with cobalt-based SiO₂ nanocomposite (Co−SiO₂) as the core and Ti-doped mesoporous silica as the shell was designed to catalyze a one-pot reaction of sulfide oxidation with in situ generated hydroperoxide. The catalyst was characterized by SEM, TEM, UV−vis spectroscopy, and XPS, among other methods. Compared to Co−SiO₂ and the physical mixture of the two components (Co−SiO₂ + Ti− Si), the core−shell catalyst significantly enhanced the reaction rate of the sulfide oxidation. The utilization efficiency of the hydroperoxide was an important factor responsible for the differences in the reaction rates. A further mechanism study showed that the improvement of the efficiency was due to the existence of a coordination pathway. The core−shell structure of a bifunctional catalyst represents a strategy for improving the utilization efficiency of hydroperoxide.

KEYWORDS: *in situ generated hydroperoxide, utilization efficiency, core−shell, oxidation reactions, mesoporous silica*
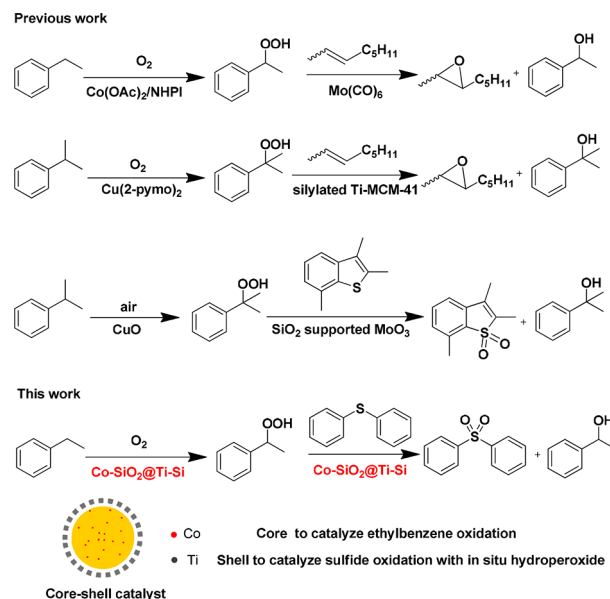
■ INTRODUCTION

The synthesis of a wide variety of valuable oxygen-containing products with atomically efficient, inexpensive, and readily available oxidants is the most economical and ecological route.[1,2] Among the various oxidants, O₂ is the most abundant and environmentally benign oxidant,[3−5] but the triplet-spin ground state makes it inert to direct utilization. Many efforts have been made to transform the O₂ into active oxygen species, for example, H₂O₂,[6,7] organic hydroperoxide,[8,9] metal−oxygen species,[10] and super oxo.[11,12] Owing to its high activity and special structure, organic hydroperoxide has attracted much attention. However, the unstable properties of organic hydroperoxide limit its utilization. In this regard, the in situ strategy has been employed to conquer this problem. The coupling of hydrocarbon oxidation and alkene oxidation was utilized for alkene epoxidation with O₂ by Ishii and co-workers[8] and Corma and co-workers,[13,14] where O₂ was converted into organic hydroperoxide by hydrocarbon oxidation.

In addition to the epoxidation of alkenes, the oxidative desulfurization of jet fuel was designed to be carried out by a two-step procedure coupled with in situ generated cumene hydroperoxide by Song and co-workers.[15,16] The above pathways are shown in Scheme 1.

The utilization of in situ generated hydroperoxide is a promising strategy for the oxidation reaction with dioxygen as the oxidant. In the aforementioned examples, the catalytic process contains two processes, namely, the formation of hydroperoxide and the oxidation of the substrate with hydroperoxide. In addition, these two steps often involve two

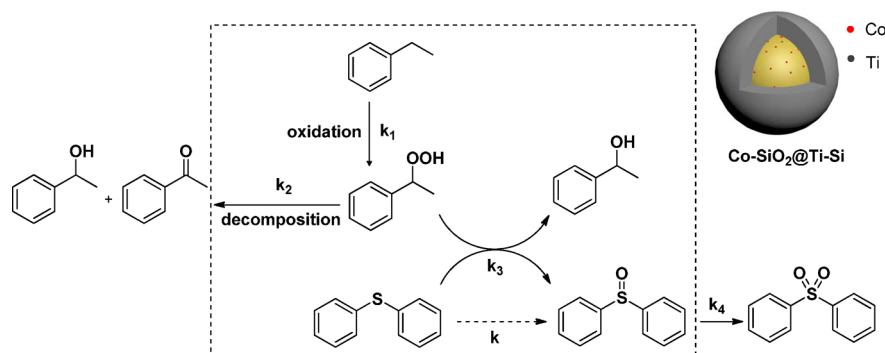**Scheme 1. Strategy of Utilizing in Situ Generated Hydroperoxide**

Scheme 2. Reaction Process of the One-Pot Aerobic Oxidation of Diphenyl Sulfide Coupled with Ethylbenzene

different catalysts. However, the hydroperoxide is very active and unstable and easily self-decomposes by a free-radical mechanism or is catalytically decomposed by metal ions,[17−20] especially at high concentration. This results in the low utilization efficiency of in situ generated hydroperoxide, meaning that much of the generated hydroperoxide does not participate in the second step. Very little attention has been paid to this issue. It is important to develop new catalysts or catalytic processes to improve the utilization efficiency of in situ generated hydroperoxide. One possible approach is to utilize the hydroperoxide as soon as it is formed. However, for such reactions to be carried out in solution, particularly for batch processes, two challenging criteria must be met. The first is that the catalyst or catalytic process should offer convenience for the hydroperoxide to contact the second active site. This means that the catalyst should minimize the distance between the two types of sites, which is called nanoscale intimacy.[21] Second, an additional selectivity screening would be necessary to prevent the exposure of the hydroperoxide, which would cause the catalytic decomposition of the hydroperoxide. To meet such design requirements, a special structured catalyst is required.

The core−shell nanostructured catalyst is a type of nanomaterial developed in recent years. Such catalysts have shown wide applications in bionanotechnology, energy storage materials, and catalytic processes, among others.[22−25] One of the attractive aspects of such materials is that they can be designed with two catalytic sites separated, enabling higher efficiency, yield, and selectivity to be achieved in catalytic applications by taking advantage of the synergism between the core and the shell,[26−29] which might be suitable for this reaction. Previously, our group reported core−shell catalysts with Au as the core and hydrophobic silica/porous organic networks as the shell to promote catalytic reactions.[30,31]

In this work, a core−shell catalyst (Co−SiO$_2$@Ti−Si) was designed, with a uniformly distributed Co−SiO$_2$ nanocomposite as the core, which promoted the formation of hydroperoxide; a mesoporous titanium silicate as the shell serves as cages for capturing the in situ formed hydroperoxide and supplying the second catalytic site to improve the substrate oxidation. Ethylbenzene was selected as the model hydrocarbon, and the oxidation of sulfide to sulfoxide and sulfone serves as the model coupled reaction. It was found that the catalyst enhanced the hydroperoxide utilization efficiency. A detailed study of the reaction process and the kinetic characteristics of the one-pot oxidation was carried out. Furthermore, a comparative study of the kinetic reaction rates and hydroperoxide utilization efficiencies was conducted among the blank, Co−SiO$_2$, Co−SiO$_2$@Ti−Si, and physically mixed

Co−SiO$_2$ with Ti-doped silica (Ti−Si) systems. To comprehend the process more clearly, an investigation of the mechanism was conducted. The reaction process is presented in Scheme 2.

■ EXPERIMENTAL SECTION

Chemicals and Materials. Tetraethyl orthosilicate (TEOS, 99%), cetyltrimethylammonium bromide (CTAB, 99%), cyclohexane (99%), ethylbenzene (99%), n-butyl alcohol (99.5%), acetonitrile (99.5%), and ammonia (28%) were obtained from Tianjin Kermel Chemical Reagent Development Center (Tianjin, China). Acetylacetone (99%) and Co(OAc)$_2$·4H$_2$O (99.5%) were purchased from Sinopharm Chemical Reagent Co., Ltd. Poly(oxyethylene) nonylphenol ether (NP-7, industrial grade) and titanium(IV) isopropoxide were purchased from Aladdin Chemicals (Shanghai, China). Diphenyl sulfide (98%) was purchased from Alfa Aesar. Diphenyl sulfoxide (98%) and diphenyl sulfone (99%) were purchased from Adamas Reagent Co. Ltd.

Catalyst Preparation. The Co−SiO$_2$ was synthesized according to our reported procedure.[32] First, a mixture of n-butyl alcohol (8.05 g), cyclohexane (35.05 g), and NP-7 (15.05 g) was added to a 250 mL bottle. Then, a mixture of Co(OAc)$_2$·4H$_2$O (0.12 g), H$_2$O (5.20 g), and NH$_3$·H$_2$O (2.00 g, 28%) were added. After the mixture had been stirred for 40 min, TEOS (5.20 g) was added slowly with stirring. After 12 h, 10 mL of acetone was added to precipitate the materials. The materials were washed with hot ethanol and dried at 353 K for 12 h. Co−SiO$_2$@Ti−Si was formed on Co−SiO$_2$. The Co−SiO$_2$ (0.5 g) was dispersed in a mixture of 150 mL of ethanol and 200 mL of H$_2$O and sonicated for 20 min. Then, 0.75 g of CTAB and 2.90 mL of NH$_3$·H$_2$O were added. After the mixture had been stirred for 10 min, titanium(IV) isopropoxide (30 mg), acetylacetone (28 mg), and TEOS (0.70 g) were added dropwise. The suspension was stirred at room temperature for 12 h. Then, the suspension was separated by centrifugation and washed with hot 6 g/L NH$_4$NO$_3$/ethanol several times. After that, it was washed with ethanol and H$_2$O and dried at 353 K overnight. The synthesis of Co−SiO$_2$@2Ti−Si followed the same procedure as used for Co−SiO$_2$@Ti−Si, except for the amounts of titanium(IV) isopropoxide (60 mg) and acetylacetone (58 mg). Except for the addition of Co−SiO$_2$, the synthesis of Ti-doped silica (Ti−Si) was the same as that of Co−SiO$_2$@Ti−Si.

1-Phenylethyl Hydroperoxide (PEHP) Synthesis. PEHP was extracted from a reaction solution of ethylbenzene autoxidation by dioxygen.[20] The reaction solution was washed with NaOH aqueous solution. Then, the aqueous phase was

mixed with plenty of NaHCO$_3$ to obtained PEHP. PEHP was extracted from the aqueous phase with *n*-hexane. Finally, the PEHP was extracted from *n*-hexane with acetonitrile.

Catalytic Reactions. The one-pot oxidation of sulfides with dioxygen was performed in a 60 mL stainless steel autoclave reactor equipped with a manometer, an automatic temperature controller, and a magnetic stirring bar. In a typical experiment, diphenyl sulfide (1 mmol), ethylbenzene (5 mL), acetonitrile (5 mL), and catalyst (50 mg) were added to the reactor. The reactor was heated to 120 °C for a certain time under 1.0 MPa O$_2$. After the reaction, the autoclave was cooled rapidly.

The catalytic oxidation of diphenyl sulfide with PEHP was conducted in Ace Glass pressure tubes. Diphenyl sulfide (0.5 mmol) and certain amounts of PEHP and catalyst were added. Then, the tubes were flushed with nitrogen for a while to remove the air. After the oil bath reached 120 °C, the tubes were placed in it and held there for the desired time.

The decomposition of PEHP was conducted in Ace Glass pressure tubes under nitrogen. In a typical procedure, 1.2 mL of acetonitrile solution containing PEHP (0.43 mmol/mL) and 3.8 mL of acetonitrile were mixed, and a certain amount of catalyst was added. The reaction was conducted for a certain time.

Product Analysis. The reaction products were analyzed with an Agilent 6890N gas chromatograph equipped with a flame ionization detector (FID) and an HP-INNOWAX column (30 m × 0.320 mm). Gas chromatography–mass spectrometry (GC–MS) analysis was carried out using an Agilent 6890N GC/5973 MS system with an HP-5MS capillary column in electrospray ionization (ESI) mode. The quantitation of products and reactant was achieved by the internal standard method using *p*-dichlorobenzene as the internal standard. The amount of PEHP consumed in the catalytic oxidation of diphenyl sulfide and the results of the decomposition of PEHP were determined by titration with Na$_2$S$_2$O$_3$.

Catalyst Characterization. Transmission electron microscopy (TEM) images were recorded on a Hitachi HT7700 microscope operating at 100 kV. Energy-dispersive X-ray (EDX) spectra were measured on a Tecnai G^2 F30S-Twin microscope. Scanning electron microscopy (SEM) images were recorded on a Hitachi S5500 microscope. N$_2$ sorption was performed on a Quantachrome Autosorb-1 and Quadrasorb SI surface area and pore size analyzer. UV–vis diffuse reflectance spectroscopy (DRS) was performed between 800 and 200 nm on a Shimadzu UV-2600 instrument. Fourier transform infrared (FT-IR) spectra were collected between 4000 and 400 cm^{-1} in KBr disks on a Bruker Tensor 27 system with a resolution of 5 cm^{-1}. Powder X-ray diffraction (XRD) patterns were recorded using an Empyrean X-ray diffractometer (PANalytical B.V.). X-ray photoelectron spectroscopy (XPS) was recorded on a Thermo ESCALAB 250Xi spectrometer. Inductively coupled plasma atomic emission spectroscopy (ICP AES) was measured on a PerkinElmer ICP-OES 7300DV instrument.

■ RESULTS AND DISCUSSION

Compositions and Properties of the Catalysts. The morphologies of the materials were determined by transmission electron microscopy (TEM) and scanning electron microscopy (SEM). As shown in Figure 1a, the Co−SiO$_2$ formed uniform spheres. Hydrolysis of tetraethyl orthosilicate and titanium(IV) isopropoxide in the presence of Co−SiO$_2$ resulted in the formation of a titanium silicate shell on the Co−SiO$_2$ spheres.
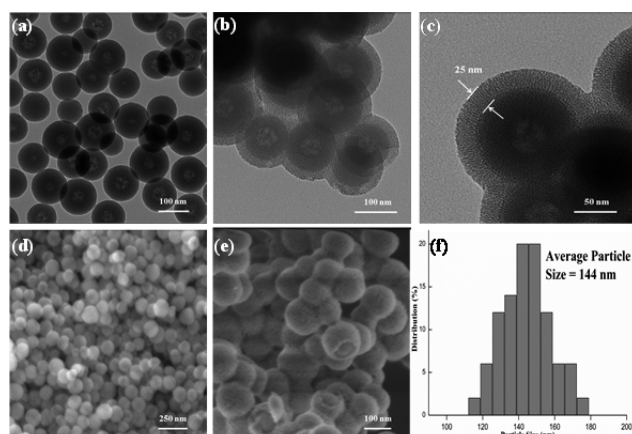

Figure 1. (a−c) TEM images of the catalysts (a) Co−SiO$_2$ and (b,c) Co−SiO$_2$@Ti−Si, (d,e) SEM images of (d) Co−SiO$_2$ and (e) Co−SiO$_2$@Ti−Si, and (f) size distribution diagram of Co−SiO$_2$@Ti−Si.
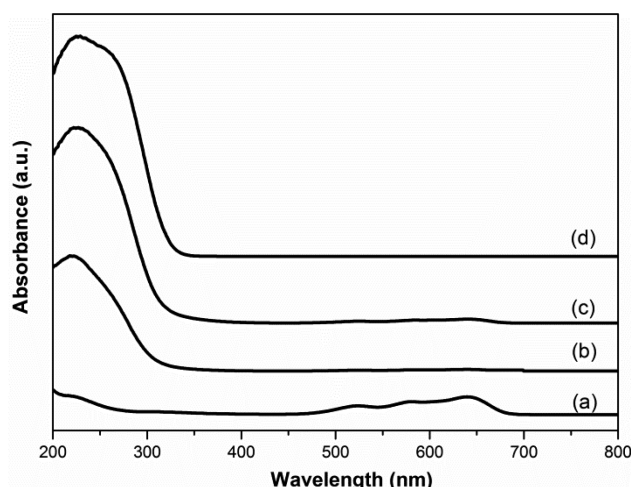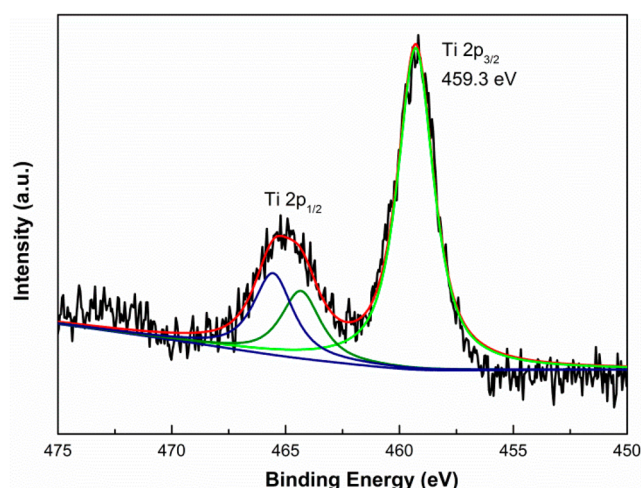
The Co−SiO$_2$@Ti−Si core−shell structure was clearly observed by TEM and SEM (Figure 1b,e). Especially from the SEM image of Co−SiO$_2$@Ti−Si, a shaggy shell that was permeable was observed, confirming the core−shell structure. The thickness of the shell was about 25 nm, and the average size of the core−shell structure was 144 nm (Figure 1c,f). As the core−shell structure was confirmed, the mesoporous structure of the shell was characterized by small-angle X-ray diffraction (XRD) measurements and N$_2$ adsorption−desorption analysis. From the XRD pattern, an obvious peak at 2θ = 2.3° appeared for the core−shell structure, but no peak appeared for the nonporous core Co−SiO$_2$ nanoparticles (Figure S3). The adsorption and desorption isotherms of the catalysts are shown in Figure S4. The Co−SiO$_2$@Ti−Si has a Brunauer−Emmett−Teller (BET) surface area (S_{BET}) of 408 m^2/g. In contrast, the surface area of Co−SiO$_2$ was 59 m^2/g, meaning that the surface area was mainly from the mesoporous shell. The S_{BET} value of Co−SiO$_2$@2Ti−Si was 406 m^2/g, and the S_{BET} value of pure Ti−Si was up to 663 m^2/g. The textural properties of the catalysts used in this work are presented in Table 1.

The state of the titanium species in the Ti-containing mesoporous silica shell was further analyzed by UV−vis DRS, which provides information about the degree of dispersion of the Ti(IV) sites on the silica shell.[33] The maximum absorption peaks of the catalysts are reported in Table 1. In addition, the entire UV−vis DRS spectra are presented in Figure 2. Three consecutive absorption peaks ranging from 450 to 750 nm were assigned to Co(II) in tetrahedral environments,[32] which is consistent with our previous work. The absorption peaks of Co also appeared in the spectrum of the core−shell catalyst. As Table 1 shows, the maximum absorption peaks of all of the samples are in the range of 210−230 nm and are attributed to isolated Ti species.[34,35] In general, isolated Ti has a coordination sphere of tetrahedral or octahedral forms.[36] The absorption peak in the range of 210−230 nm was attributed to a ligand-to-metal charge-transfer band for O^{2-} to Ti^{4+}, which is a characteristic of tetrahedrally coordinated Ti.[37,38] This implies that the catalysts contained mainly tetrahedral Ti species.

The oxidation states of titanium were further identified by X-ray photoelectron spectroscopy (XPS). The deconvolution of the Ti 2p spectrum for Co−SiO$_2$@Ti−Si is shown in Figure 3, which displays a binding energy (BE) of 459.3 eV for Ti 2p$_{3/2}$. According to previous reports, the BE of Ti 2p$_{3/2}$ for
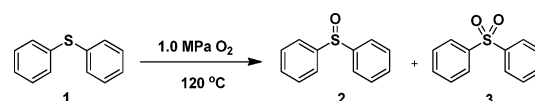
Table 1. Textural Properties and Related Metal Content of the Synthesized Catalysts

| | ICP AES | | | | | |
catalyst	Co (wt %)	Ti (wt %)	S_{BET} (m^2/g)	V_p (cm^3 g^{-1})	D_p (nm)	UV max (nm)
Co—SiO$_2$	1.87	–	59	–	–	640
Co—SiO$_2$@Ti—Si	1.32	0.85	408	0.39	2.2	222
Co—SiO$_2$@2Ti—Si	1.28	1.45	406	0.59	2.5	225
Ti—Si	–	2.14	663	0.49	–	226

Figure 2. UV–vis DRS spectra of the catalysts (a) Co–SiO$_2$, (b) Co–SiO$_2$@Ti–Si, (c) Co–SiO$_2$@2Ti–Si, and (d) Ti–Si.

Figure 3. Ti 2p XPS spectra of the catalyst Co–SiO$_2$@Ti–Si.

extraframework Ti(IV) is 457.8 ± 0.2 eV.[39] The higher BE of Co–SiO$_2$@Ti–Si (459.3 eV) was attributed to Ti(IV) in tetrahedral coordination, implying that no extraframework Ti(IV) existed in the core–shell catalyst.[40−42] This is in accordance with the UV–vis DRS results.

Catalytic Oxidation of Aromatic Sulfides. The catalytic performances of the as-synthesized catalysts were analyzed in the one-pot oxidation of diphenyl sulfide in acetonitrile as the model reaction. Ethylbenzene is believed to react with dioxygen to generate 1-phenethyl hydroperoxide (PEHP) as the oxidant to convert sulfide into sulfoxide and sulfone. Reactions in the absence of ethylbenzene gave no activity in the systems (Table 2, entries 1−3). The conversions were markedly improved by the addition of ethylbenzene (Table 2, entries 4−6), and an obvious advantage in performing diphenyl sulfide conversion

Table 2. Aerobic Oxidation of Diphenyl Sulfide[a]

| | | | conversion (%) | product distribution (%) | |
entry	catalyst	solvent		2	3
1[b]	–	CH$_3$CN	–	–	–
2[b]	Co–SiO$_2$	CH$_3$CN	–	–	–
3[b]	Co–SiO$_2$@Ti–Si	CH$_3$CN	–	–	–
4	–	CH$_3$CN	44	98	2
5	Co–SiO$_2$	CH$_3$CN	69	83	17
6	Co–SiO$_2$@Ti–Si	CH$_3$CN	99	0	>99
7[c]	Co–SiO$_2$@Ti–Si	CH$_3$CN	74	71	29
8[c]	Co–SiO$_2$@Ti–Si	MeOH	39	98	2
9[c]	Co–SiO$_2$@Ti–Si	DCE	22	86	14
10[c]	Co–SiO$_2$@Ti–Si	DMF	20	>99	0

[a]Reaction conditions: 1 mmol of substrate, 5 mL of ethylbenzene, 5 mL of CH$_3$CN as the solvent, 50 mg of catalyst, 4 h. [b]10 mL of CH$_3$CN, without ethylbenzene; [c]5 mL of solvent, 5 mL of ethylbenzene, 2 h.

over Co–SiO$_2$@Ti–Si (99%) rather than in the blank system (44%) and over Co–SiO$_2$ (69%) was observed. In terms of solvents, methanol (MeOH), 1,2-dichloroethane (DCE), and dimethylformamide (DMF) were tested. Acetonitrile showed the best catalytic activity among these solvents (Table 2, entries 7–10), which could be ascribed to the good performance of ethylbenzene oxidation in acetonitrile.[43] In addition, kinetic studies on the one-pot oxidation of diphenyl sulfide were carried out. The kinetic reaction rates (k) were determined by the decreasing concentration of diphenyl sulfide. A good linear relationship was found for the linear fit of $\ln(C_t/C_0)$ against the reaction time, which demonstrates pseudo-first-order kinetics (Figure S7). As shown in Figure 4, the reaction rate of Co–
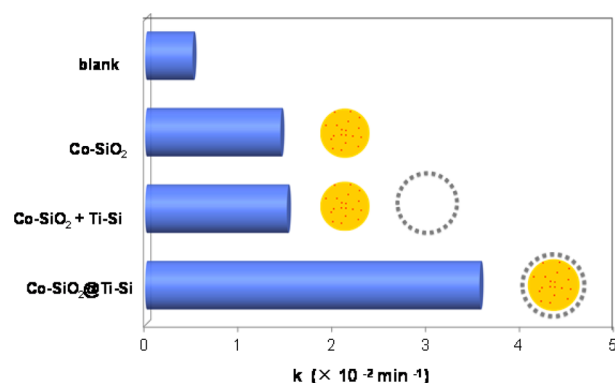

Figure 4. Kinetics of the one-pot oxidation of diphenyl sulfide.

SiO_2 (14.4×10^{-3} min^{-1}) was superior to that of the blank (5.0×10^{-3} min^{-1}), whereas the physically mixed Co−SiO$_2$ and Ti−Si (Co−SiO$_2$ + Ti−Si) achieved a slight higher reaction rate (15.1×10^{-3} min^{-1}) than Co−SiO$_2$, which means that physical mixing as a way of introducing Ti−Si to improve the reaction rate is valid but also limited. Interestingly, a marked increase in k was achieved for Co−SiO$_2$@Ti−Si (35.6×10^{-3} min^{-1}), which contained the same amounts of Co and Ti as the physical mixture. In other words, the method of combining Co−SiO$_2$ and Ti−Si as a core−shell structure instead of physically mixing them significantly increased the reaction rate, which was attributed to the advantage of nanoscale intimacy. Overall, the above results verified the validity of the preliminary design of the bifunctional core−shell catalyst to some extent.

Intermediates in the Catalytic Aerobic Oxidation of Diphenyl Sulfide. A study of the intermediates in the reaction process was subsequently conducted. As mentioned previously, the PEHP from ethylbenzene oxidation was the oxidant. To confirm this issue, a separated PEHP material was synthesized. The blank, Co−SiO$_2$, and Co−SiO$_2$@Ti−Si system all showed a certain amount of conversion upon the addition of PEHP (Table 3, entries 2−4), whereas diphenyl sulfoxide and

Table 3. Oxidation of Diphenyl Sulfide with PEHP[a]

entry	catalyst	conversion (%)[b]	yield (%)	
			2	**3**
1[c]	blank	−	−	−
2[d]	blank	5	5	0
3[d]	Co−SiO$_2$	7	7	0
4	Co−SiO$_2$@Ti−Si	34	29	1
5	Co−SiO$_2$ + Ti−Si	25	21	3
6	Co−SiO$_2$@2Ti−Si	69	53	14
7[e]	Co−SiO$_2$@Ti−Si	47	37	7

[a]Reaction conditions: 0.5 mmol of diphenyl sulfide, 5 mL of CH$_3$CN, 0.51 mmol of PEHP, 120 °C, 2 h, N$_2$. [b]Conversion of **1**. [c]No PEHP. [d]Conversion was determined by sum of the products. [e]50 mg of catalyst.

diphenyl sulfone were not detected without PEHP (Table 3, entry 1). This suggests that PEHP was the oxidant originating from the oxidation of ethylbenzene. Upon analysis of the product distribution during the reaction process through online sampling of the Co−SiO$_2$@Ti−Si system (Figure 5), an accumulation of diphenyl sulfoxide in the early reaction stage and a sharp decrease when the conversion reached nearly 70% were observed; meanwhile, an increase in diphenyl sulfone emerged. This suggests that diphenyl sulfoxide might be the intermediate and might finally be converted to diphenyl sulfone. To verify this conclusion, a kinetic study was conducted of the one-pot oxidation with diphenyl sulfoxide as the reactant. Diphenyl sulfoxide was converted to diphenyl sulfone with the kinetic reaction rates (k_4) displayed in Figure 6c. Compared to the k value determined for Co−SiO$_2$@Ti−Si (35.6×10^{-3} min^{-1}), k_4 (15.0×10^{-3} min^{-1}) was much lower, which led to the accumulation of diphenyl sulfoxide. Hence, diphenyl sulfoxide was confirmed as the intermediate.
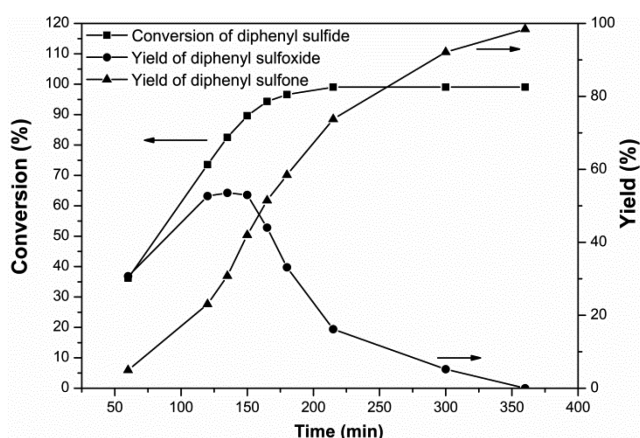

Figure 5. Time course of the catalytic conversion of diphenyl sulfide over Co−SiO$_2$@Ti−Si.

Formation and Utilization of PEHP in the Catalytic Oxidation Process. The relatively better performance of Co−SiO$_2$@Ti−Si for the title reaction was confirmed in an earlier description, and PEHP was the oxidant, so an investigation based on the formation and utilization of PEHP was conducted to investigate the reasons. Based on the aforementioned reaction process shown in Scheme 2, exploratory experiments were designed. The oxidation of ethylbenzene (with rate constant k_1), which generated PEHP, was first analyzed through a kinetic study without diphenyl sulfide. As shown in Figure 6a, the kinetic reaction rates (k_1) of Co−SiO$_2$ (4.6×10^{-3} min^{-1}) and Co−SiO$_2$@Ti−Si (5.7×10^{-3} min^{-1}) exhibited little difference, which should generate comparable amounts of PEHP. The blank system (1.6×10^{-3} min^{-1}) was inferior to both catalysts. The marked increase in k for Co−SiO$_2$@Ti−Si compared to Co−SiO$_2$ cannot be attributed to the differences in k_1. For the decomposition of PEHP (k_2), separate PEHP was used as a reactant to undergo contrast experiments.

Co−SiO$_2$@Ti−Si exhibited a higher decomposition rate than the other systems (Figure 6b), showing that k_2 also cannot account for the superiority of Co−SiO$_2$@Ti−Si. Excluding the key influence of differences in k_1 and k_2, it is worth noting the utilization efficiency of PEHP, which might be the key factor. Here, the utilization efficiency of PEHP (Eff$_{PEHP}$) represents the proportion of PEHP used, of the overall amount consumed, that converted sulfide to sulfoxide and sulfone. This was determined through an experiment with separate PEHP as the oxidant for diphenyl sulfide oxidation. The blank, Co−SiO$_2$, and Co−SiO$_2$@Ti−Si systems all showed a certain amount of conversion (Table 3, entries 2−4). The conversions for the blank and Co−SiO$_2$ systems were 5% and 7%, respectively. Co−SiO$_2$@Ti−Si achieved a conversion of 34%, which suggested an overwhelming advantage at converting diphenyl sulfide. The corresponding results for Eff$_{PEHP}$ are displayed in Figure 6d. The Eff$_{PEHP}$ values of Co−SiO$_2$ and the blank were inferior to that of Co−SiO$_2$@Ti−Si. Compared with the physical mixture of Co−SiO$_2$ and Ti−Si, Co−SiO$_2$@Ti−Si also achieved higher Eff$_{PEHP}$ values. For the title reaction, when a given amount of PEHP was used as the oxidant, higher Eff$_{PEHP}$ represents more available oxidant, which would bring a higher conversion and reaction rate. Hence, the higher Eff$_{PEHP}$ of Co−SiO$_2$@Ti−Si indicates its better performance.

A catalyst containing a double content of titanium was synthesized (Co−SiO$_2$@2Ti−Si), which maintained the core−shell structure and mesoporous shell with Ti(IV) in tetrahedral
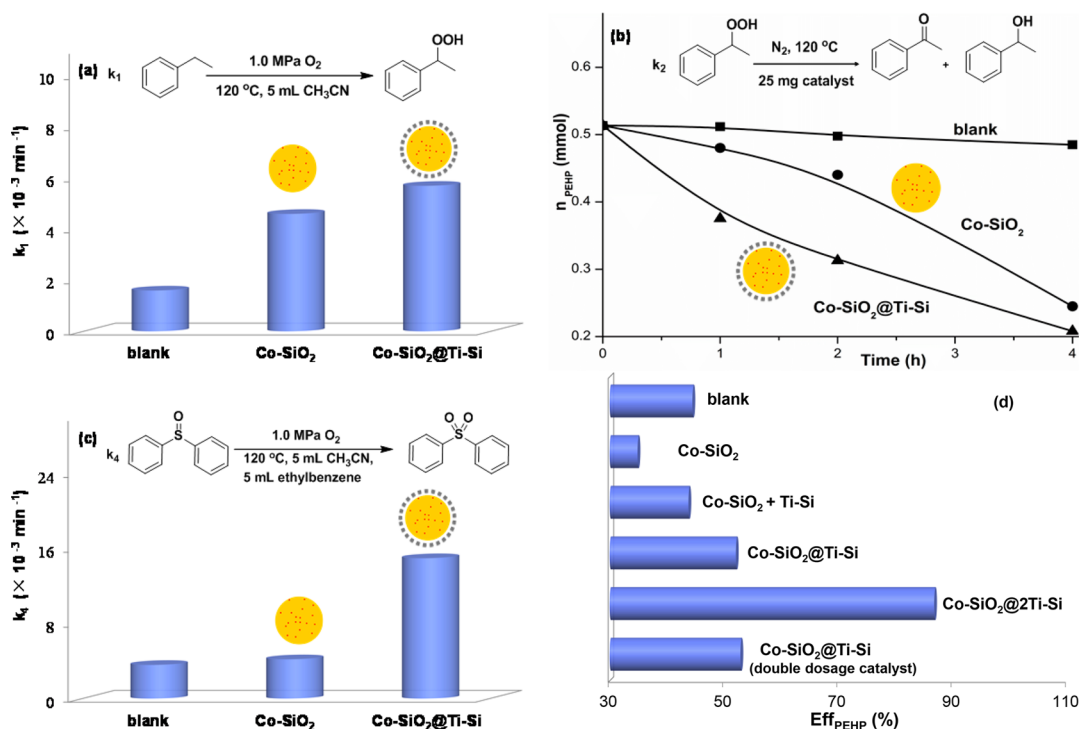
Figure 6. Kinetic study of each step in the one-pot oxidation: (a) oxidation rate of ethylbenzene, (b) decomposition regularity of PEHP, (c) oxidation rate of diphenyl sulfoxide to sulfone, and (d) comparative PEHP utilization efficiencies (Eff_{PEHP} values) of the catalysts.

coordination (Figure S1, Table 1). When Co−SiO$_2$@2Ti−Siwas used in the reaction with PEHP, a remarkable result was attained. Compared with Co−SiO$_2$@Ti−Si, the conversion of diphenyl sulfide increased from 34% to 69% (Table 3, entries 4 and 6), and the corresponding Eff_{PEHP} increased from 52% to 87% (Figure 6d). In contrast, a double dosage of Co−SiO$_2$@Ti−Si was added, which achieved an Eff_{PEHP} value of 53%, nearly the same as the 52% for Co−SiO$_2$@Ti−Si with half as much Ti (Figure 6d). This confirms that Co−SiO$_2$@2Ti−Si was more efficient, not only because of its high Ti content but also because of the rational design of the core−shell components.

Scope of Aromatic Sulfides and Hydrocarbons. Because of the excellent performance of the core−shell bifunctional Co−SiO$_2$@Ti−Si catalyst in the one-pot oxidation of the model reaction, a structurally diverse set of sulfides and hydrocarbons were studied under similar conditions. As can be seen in Table 4, the substituent groups of the sulfides had little effect on the conversion. The alkyl aromatics with methylene were qualified for the oxidation (entries 4−6). Unlike the other three hydrocarbons, tetralin achieved a relatively poor conversion of diphenyl sulfide (entry 6), which might be due to steric effects.

Mechanism Analysis of the High PEHP Utilization Efficiency of Co−SiO$_2$@Ti−Si. Based on the above discussion, the PEHP utilization efficiency was confirmed as an important factor influencing the reaction rate of diphenyl sulfide. Exploratory experiments aimed at comprehending the process more clearly and investigating the reasons for the higher Eff_{PEHP} value for Co−SiO$_2$@Ti−Si were conducted. For the one-pot reaction with ethylbenzene and diphenyl sulfide, the addition of free-radical inhibitor of 2,6-di-tert-butyl-4-methylphenol (BHT) completely stopped the oxidation of sulfide for the blank and Co−SiO$_2$ systems, whereas Co−SiO$_2$@Ti−Si still achieved a 17% conversion, which can be

attributed to the effective PEHP utilization (Figure 7a). In general, ethylbenzene oxidation usually undergoes a free-radical process,[43,44] which would be stopped by BHT. Thus, to further confirm that the oxidation of diphenyl sulfide is a free-radical process, a suitable amount of BHT was added to the reaction system that used PEHP as the oxidant without any ethylbenzene. The addition of BHT had a marked influence on the blank and Co−SiO$_2$ systems, which showed obvious decreases in conversion, from 47% to 17% and from 52% to 18% for the blank and Co−SiO$_2$ systems, respectively (Figure 7b).

However, the Co−SiO$_2$@Ti−Si system showed a decrease in the conversion of diphenyl sulfide from 84% to 80%, which was nearly not influenced by BHT. This means that the blank and Co−SiO$_2$ systems mainly go through free-radical processes, whereas the Co−SiO$_2$@Ti−Si system did not exhibit a typical free-radical process. Based on previous reports, titanium silicate and hydroperoxide are apt to form a coordinated complex to realize the catalytic process.[45,46] PEHP was thus mixed with Co−SiO$_2$@2Ti−Si, and the mixture was characterized by the UV−vis DRS. As shown in Figure 8, the peak for Ti(IV) shifted from 224 nm to peaks at 243 and 282 nm. As reported, a coordination sphere of Ti (tetrahedral or octahedral) and the number of bonds to the silica surface can lead to a shift of the peak.[47] In particular, the 282 nm peak was attributed to octahedral Ti species.[36] Thus, this confirmed that PEHP and Co−SiO$_2$@2Ti−Si formed a coordinated complex to some extent. According to the two parts of analysis, for the blank and Co−SiO$_2$ systems, PEHP was decomposed into active radicals to stimulate diphenyl sulfide oxidation through a radical process. In contrast, because of the introduction of Ti, in addition to the radical process observed in the blank and Co−SiO$_2$ systems, Co−SiO$_2$@Ti−Si catalyzed the diphenyl sulfide oxidation mainly through the coordinated pathway. Hence, the high PEHP utilization efficiency of Co−SiO$_2$@Ti−Si can be

Table 4. Catalytic Aerobic Oxidation of Structurally Diverse Sulfides with Methylene Hydrocarbons over Co−SiO₂@Ti−Si[a]

entry	sulfide	hydrocarbon	conversion (%)[b]	product distribution (%)	
				1	2
1			95	32	68
2			98	5	95
3			98	0	>99
4			99	0	>99
5			99	0	>99
6[c]			73	86	14

[a]Reaction conditions: 1 mmol of sulfide, 5 mL of CH₃CN, 5 mL of hydrocarbon, 50 mg of catalyst, 120 °C, 4 h, 1.0 MPa O₂. [b]Conversion of sulfide. [c]100 °C, 0.5 MPa O₂, 4 h.

attributed to the existence of an effective coordinated pathway. A possible mechanism is proposed in Scheme 3.
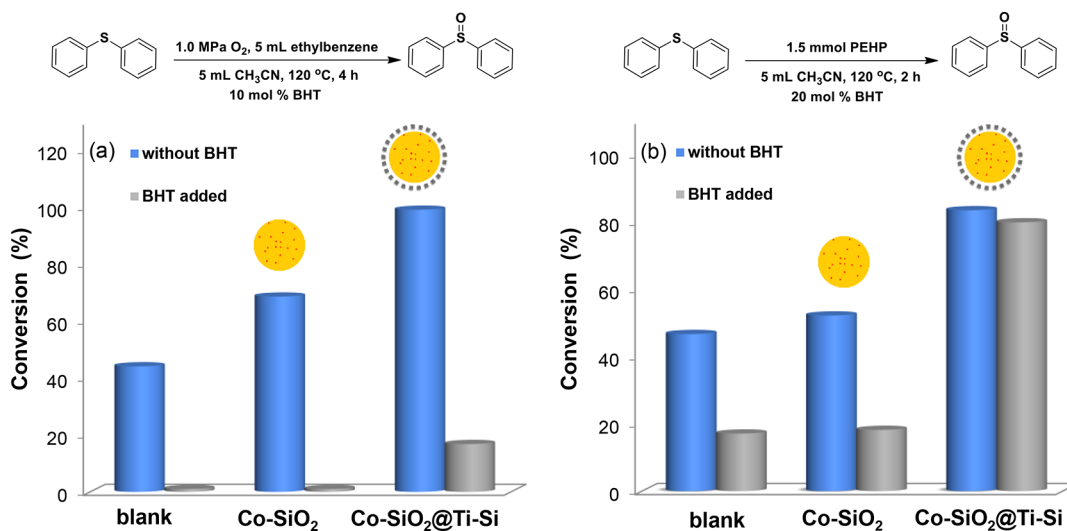

Figure 8. UV−vis DRS spectra of Co−SiO₂@Ti−Si mixed with PEHP.

Scheme 3. Proposed Mechanism for the Title Reaction

Figure 7. Effects of BHT on the oxidation of diphenyl sulfide (a) with ethylbenzene addition and (b) with PEHP as the oxidant.

CONCLUSIONS

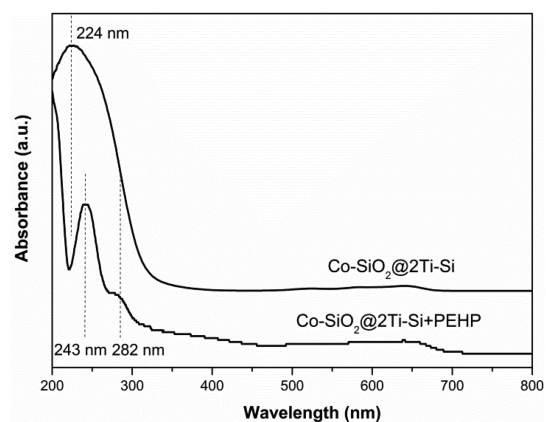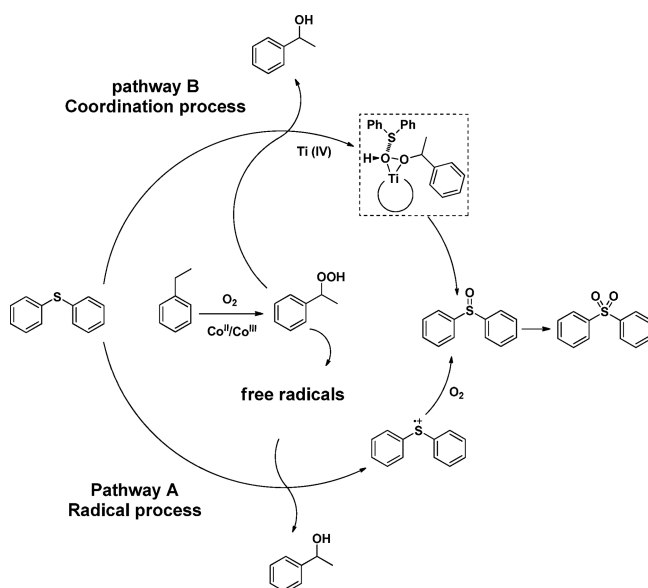To summarize, we have designed a bifunctional core−shell catalyst for the one-pot oxidation of sulfide coupled with hydrocarbon oxidation. The core−shell structured method of combining Co−SiO$_2$ and Ti−Si proved to be an effective strategy for utilizing the in situ generated hydroperoxide. A kinetic study was carried out, and the reasons for the differences in the kinetic reaction rates over Co−SiO$_2$@Ti−Si and comparative catalytic systems were explored. The PEHP utilization efficiency was an important factor in the superiority of Co−SiO$_2$@Ti−Si. The relatively higher PEHP utilization efficiency of Co−SiO$_2$@Ti−Si was attributed to the different main way in which it is utilized, which was promoted by the introduction of Ti species and the effective method of combining Co−SiO$_2$ and Ti−Si in a core−shell structure. A coordination mechanism of Ti-containing catalyst with PEHP was preliminarily determined. The core−shell structure of a bifunctional catalyst represents a way of improving the utilization efficiency of hydroperoxide in the one-pot oxidation. A further investigation of extended applications of in situ generated hydroperoxide is currently underway in our group.

ASSOCIATED CONTENT

Ⓢ Supporting Information

The Supporting Information is available free of charge on the ACS Publications Web site. The Supporting Information is available free of charge on the ACS Publications website at DOI: 10.1021/acscatal.7b03259.

Characterization data and relative kinetics data (PDF)

AUTHOR INFORMATION

Corresponding Authors

*E-mail: xujie@dicp.ac.cn.
*E-mail: shisong@dicp.ac.cn.

ORCID Ⓞ

Min Wang: 0000-0002-9072-8331
Jie Xu: 0000-0003-2535-094X

Notes

The authors declare no competing financial interest.

ACKNOWLEDGMENTS

REFERENCES

(1) Sheldon, R. A.; Downing, R. S. *Appl. Catal., A* **1999**, *189*, 163−183.

(2) Matsumoto, T.; Ueno, M.; Wang, N.; Kobayashi, S. *Chem. - Asian J.* **2008**, *3*, 196−214.

(3) Mallat, T.; Baiker, A. *Chem. Rev.* **2004**, *104*, 3037−3058.

(4) Vedernikov, A. N. *Acc. Chem. Res.* **2012**, *45*, 803−813.

(5) Guo, Z.; Liu, B.; Zhang, Q.; Deng, W.; Wang, Y.; Yang, Y. *Chem. Soc. Rev.* **2014**, *43*, 3480−3524.

(6) Sheriff, T. S.; Cope, S.; Varsani, D. S. *Dalton Trans.* **2013**, *42*, 5673−5681.

(7) Limvorapitux, R.; Chou, L.-Y.; Young, A. P.; Tsung, C.-K.; Nguyen, S. T. *ACS Catal.* **2017**, *7*, 6691−6698.

(8) Iwahama, T.; Hatta, G.; Sakaguchi, S.; Ishii, Y. *Chem. Commun.* **2000**, 163−164.

(9) Scotti, N.; Ravasio, N.; Zaccheria, F.; Psaro, R.; Evangelisti, C. *Chem. Commun.* **2013**, *49*, 1957−1959.

(10) Aboelella, N. W.; Kryatov, S. V.; Gherman, B. F.; Brennessel, W. W.; Young, V. G., Jr.; Sarangi, R.; Rybak-Akimova, E. V.; Hodgson, K. O.; Hedman, B.; Solomon, E. I.; Cramer, C. J.; Tolman, W. B. *J. Am. Chem. Soc.* **2004**, *126*, 16896−16911.

(11) Tang, N.; Zhang, Y.; Lin, F.; Lu, H.; Jiang, Z.; Li, C. *Chem. Commun.* **2012**, *48*, 11647−11649.

(12) Tang, N.; Jiang, Z.; Li, C. *Green Chem.* **2015**, *17*, 817−820.

(13) Aprile, C.; Corma, A.; Domine, M. E.; Garcia, H.; Mitchell, C. *J. Catal.* **2009**, *264*, 44−53.

(14) Luz, I.; León, A.; Boronat, M.; Llabrés i Xamena, F. X.; Corma, A. *Catal. Sci. Technol.* **2013**, *3*, 371−379.

(15) Sundararaman, R.; Ma, X.; Song, C. *Ind. Eng. Chem. Res.* **2010**, *49*, 5561−5568.

(16) Sundararaman, R.; Song, C. *Ind. Eng. Chem. Res.* **2014**, *53*, 1890−1899.

(17) Sun, Z.; Xu, J.; Du, Z.; Zhang, W. *Appl. Catal., A* **2007**, *323*, 119−125.

(18) Wang, M.; Ma, J.; Chen, C.; Zheng, X.; Du, Z.; Xu, J. *J. Mater. Chem.* **2011**, *21*, 12609−12612.

(19) Zheng, X.; Wang, M.; Sun, Z.; Chen, C.; Ma, J.; Xu, J. *Catal. Commun.* **2012**, *29*, 149−152.

(20) Zheng, X.; Wang, M.; Sun, Z.; Liu, J.; Ma, J.; Xu, J. *Catal. Commun.* **2013**, *40*, 55−58.

(21) Zecevic, J.; Vanbutsele, G.; de Jong, K. P.; Martens, J. A. *Nature* **2015**, *528*, 245−248.

(22) Gawande, M. B.; Goswami, A.; Asefa, T.; Guo, H.; Biradar, A. V.; Peng, D. L.; Zboril, R.; Varma, R. S. *Chem. Soc. Rev.* **2015**, *44*, 7540−7590.

(23) Barmatova, M. V.; Ivanchikova, I. D.; Kholdeeva, O. A.; Shmakov, A. N.; Zaikovskii, V. I.; Mel'gunov, M. S. *Catal. Lett.* **2009**, *127*, 75−82.

(24) Wang, L.; Wang, G.; Zhang, J.; Bian, C.; Meng, X.; Xiao, F. *Nat. Commun.* **2017**, *8*, 15240.

(25) Zhang, J.; Wang, L.; Shao, Y.; Wang, Y.; Gates, B.; Xiao, F. *Angew. Chem., Int. Ed.* **2017**, *56*, 9747−9751.

(26) Wang, D.; Li, Y. *Adv. Mater.* **2011**, *23*, 1044−1060.

(27) Okada, S.; Mori, K.; Kamegawa, T.; Che, M.; Yamashita, H. *Chem. - Eur. J.* **2011**, *17*, 9047−9051.

(28) Okada, S.; Ikurumi, S.; Kamegawa, T.; Mori, K.; Yamashita, H. *J. Phys. Chem. C* **2012**, *116*, 14360−14367.

(29) Kuwahara, Y.; Ando, T.; Kango, H.; Yamashita, H. *Chem. - Eur. J.* **2017**, *23*, 380−389.

(30) Shi, S.; Wang, M.; Chen, C.; Gao, J.; Ma, H.; Ma, J.; Xu, J. *Chem. Commun.* **2013**, *49*, 9591−9593.

(31) Shi, S.; Chen, C.; Wang, M.; Ma, J.; Ma, H.; Xu, J. *Chem. Commun.* **2014**, *50*, 9079−9082.

(32) Chen, C.; Shi, S.; Wang, M.; Ma, H.; Zhou, L.; Xu, J. *J. Mater. Chem. A* **2014**, *2*, 8126−8134.

(33) Maksimchuk, N. V.; Ivanchikova, I. D.; Ayupov, A. B.; Kholdeeva, O. A. *Appl. Catal., B* **2016**, *181*, 363−370.

(34) Wang, J.; Lu, J.; Yang, J.; Chen, R.; Zhang, Y.; Yin, D.; Wang, J. *Appl. Surf. Sci.* **2013**, *283*, 794−801.

(35) Feng, X.; Sheng, N.; Liu, Y.; Chen, X.; Chen, D.; Yang, C.; Zhou, X. *ACS Catal.* **2017**, *7*, 2668−2675.

(36) Fraile, J. M.; García, N.; Mayoral, J. A.; Santomauro, F. G.; Guidotti, M. *ACS Catal.* **2015**, *5*, 3552−3561.

(37) Marchese, L.; Gianotti, E.; Dellarocca, V.; Maschmeyer, T.; Rey, F.; Coluccia, S.; Thomas, J. M. *Phys. Chem. Chem. Phys.* **1999**, *1*, 585−592.

(38) Jappar, N.; Xia, Q.; Tatsumi, T. *J. Catal.* **1998**, *180*, 132−141.

(39) Hasegawa, Y.; Ayame, A. *Catal. Today* **2001**, *71*, 177−187.

(40) Sudhakar Reddy, J.; Sayari, A. *Stud. Surf. Sci. Catal.* **1995**, *94*, 309−316.

(41) Wang, X.; Zhang, X.; Wang, Y.; Liu, H.; Wang, J.; Qiu, J.; Ho, H. L.; Han, W.; Yeung, K. L. *Chem. Eng. J.* **2011**, *175*, 408−416.

(42) Zhong, W.; Qiao, T.; Dai, J.; Mao, L.; Xu, Q.; Zou, G.; Liu, X.; Yin, D.; Zhao, F. *J. Catal.* **2015**, *330*, 208−221.

(43) Yang, G.; Ma, Y.; Xu, J. *J. Am. Chem. Soc.* **2004**, *126*, 10542−10543.

(44) Shi, S.; Liu, M.; Zhao, L.; Wang, M.; Chen, C.; Gao, J.; Xu, J. *Chem. - Asian J.* **2017**, *12*, 2404−2409.

(45) Skobelev, I. Y.; Zalomaeva, O. V.; Kholdeeva, O. A.; Poblet, J. M.; Carbo, J. J. *Chem. - Eur. J.* **2015**, *21*, 14496−14506.

(46) Sankar, G.; Thomas, J. M.; Catlow, C. R. A.; Barker, C. M.; Gleeson, D.; Kaltsoyannis, N. *J. Phys. Chem. B* **2001**, *105*, 9028−9030.

(47) Fraile, J.; Garcia, J.; Mayoral, J.; Vispe, E. *J. Catal.* **2005**, *233*, 90−99.